



Communication

Quantitative Evaluation of Burn Injuries Based on Electrical Impedance Spectroscopy of Blood with a Seven-Parameter Equivalent Circuit

Huilu Bao ¹, Jianping Li ^{1,*}, Jianming Wen ¹, Li Cheng ¹, Yili Hu ¹, Yu Zhang ¹, Nen Wan ¹ and Masahiro Takei ²

- ¹ The Institute of Precision Machinery and Smart Structure, College of Engineering, Zhejiang Normal University, Jinhua 321004, China; baohuilu@zjnu.edu.cn (H.B.); wjming@zjnu.cn (J.W.); chenglizjnu@foxmail.com (L.C.); huyili@zjnu.edu.cn (Y.H.); zjnuzy@zjnu.cn (Y.Z.); wannen@zjnu.cn (N.W.)
- ² Graduate School of Mechanical Engineering, Division of Artificial System Science, Chiba University, 1-33 Yayoi, Inage, Chiba 263-8522, Japan; masa@chiba-u.jp
- * Correspondence: lijip@zjnu.cn

Abstract: A quantitative and rapid burn injury detection method has been proposed based on the electrical impedance spectroscopy (EIS) of blood with a seven-parameter equivalent circuit. The degree of burn injury is estimated from the electrical impedance characteristics of blood with different volume proportions of red blood cells (RBCs) and heated red blood cells (HRBCs). A quantitative relationship between the volume portion H_{HCT} of HRBCs and the electrical impedance characteristics of blood has been demonstrated. A seven-parameter equivalent circuit is employed to quantify the relationship from the perspective of electricity. Additionally, the traditional Hanai equation has been modified to verify the experimental results. Results show that the imaginary part of impedance Z_{Imt} under the characteristic frequency (f_c) has a linear relationship with H_{HCT} which could be described by $Z_{Imt} = -2.56H_{HCT} - 2.01$ with a correlation coefficient of 0.96. Moreover, the relationship between the plasma resistance R_p and H_{HCT} is obtained as $R_p = -7.2H_{HCT} + 3.91$ with a correlation coefficient of 0.96 from the seven-parameter equivalent circuit. This study shows the feasibility of EIS in the quantitative detection of burn injury by the quantitative parameters Z_{Imt} and R_p , which might be meaningful for the follow-up clinical treatment for burn injury.

Keywords: burn injury; electrical impedance spectroscopy; blood; red blood cell



Citation: Bao, H.; Li, J.; Wen, J.; Cheng, L.; Hu, Y.; Zhang, Y.; Wan, N.; Takei, M. Quantitative Evaluation of Burn Injuries Based on Electrical Impedance Spectroscopy of Blood with a Seven-Parameter Equivalent Circuit. *Sensors* **2021**, *21*, 1496. <https://doi.org/10.3390/s21041496>

Academic Editor: Pedro Estrela

Received: 20 January 2021

Accepted: 17 February 2021

Published: 21 February 2021

Publisher's Note: MDPI stays neutral with regard to jurisdictional claims in published maps and institutional affiliations.



Copyright: © 2021 by the authors. Licensee MDPI, Basel, Switzerland. This article is an open access article distributed under the terms and conditions of the Creative Commons Attribution (CC BY) license (<https://creativecommons.org/licenses/by/4.0/>).

1. Introduction

It is reported that about 11 million people suffer from burn injuries every year all around the world [1–3]. The diagnosis of burn injury degrees which could provide an important reference for clinical treatment has always been an important part of burn injury studies. The quantitative measurement of burn injury is still a hot topic in the fields of research and clinical treatment.

Nowadays, some methods have been developed by researchers to measure the degrees of burn injury. The observation method is one of the most common utilized methods with an advantage of low cost [4]. However, since it is measured by the eyes of doctors, the result is greatly influenced by personal experience which may lead to a low accuracy [5]. The pathological biopsy method (PB) is another method which means the removal of diseased tissue, and its accuracy is generally high. Nevertheless, it brings harm to patients' body, and it also takes a long time to determine the degrees of burn injury [6,7]. Sometimes, other methods, like fluorescence detection (FD), infrared thermal imaging (ITI), ultrasonic imaging (UI) and computed tomography (CT) are also applied for the measurement of burn injury. However, all these methods have their own advantages and disadvantages [4,5,8,9]. New methods with high efficiency, high speed, low cost and less body harm are still necessary to be investigated to save the life and time of patients with burn injury.

In recent years, the EIS method has gained the attention of researchers for its rapid speed, non-invasive and low cost measurement characteristics [10–14]. It has been confirmed that EIS is sensitive to the microscopic compositions of cells and proteins (such as concentration, cell size, survival state) by measuring the variation of electrical impedance characteristics [15,16]. EIS has been utilized in many aspects of medical monitoring, such as the thrombus detection [17]; myoglobin detection [18]; circulating tumor cell detection [19]; status of tissue or cell detection [20,21]. It is reported that the membrane of heated red blood cells (HRBCs) is destroyed in patients with burn injury, and different degrees of burn injury lead to different proportions of red blood cells (RBCs) and HRBCs which causes the variation of blood's electrical impedance characteristics [22]. Wu et al. [23] pointed out that the hematocrit (*HCT*) increased as the patients gradually recovered. Therefore, it is feasible to exploit EIS method to determine the degrees of burn injury by measuring the impedance of blood with different *HCT* and the hematocrit of HRBCs (H_{HCT}). Nevertheless, how to quantitatively evaluate the degrees of burn injury by EIS method, and which parameters are suitable for the quantitative measurement are still unknown to the real application.

In this study, to explore a new method for burn injury detection and investigate the effective parameters, a quantitative and rapid measurement has been proposed based on EIS method by detecting the proportion of HRBCs. The content of this paper is as the following: in Section 2, an experiment system is built up to detect the electrical impedance characteristics of blood with different *HCT* and H_{HCT} . In Section 3, a seven-parameter equivalent circuit is employed to quantify the relationship from the perspective of electricity. Additionally, the conventional Hanai equation has been modified to quantify the relationship. This study might be meaningful to a more efficient, economical and rapid burn injury detection method.

2. Experiment

2.1. Experimental Setup

The experimental setup for the burn injury detection by EIS method is shown in Figure 1a. It mainly consists of a cuvette, an impedance analyzer (IM7581, Hioki E.E. Corporation, Nagano-ken, Japan) with a fixture (16092A, Agilent Technologies Inc., Palo Alto, CA, USA), and a personal computer (PC). In the experimental setup, blood is put inside the cuvette with two electrodes which are fabricated by copper. The structural dimension parameters of the cuvette are 12 mm × 12 mm × 45 mm, and the size of the electrodes in the cuvette is 10 mm × 20 mm with a distance of 2 mm, as is shown in Figure 1b. During the experiment, the impedance analyzer is utilized to measure the electrical impedance parameters of blood with the cuvette fixed in the fixture. The PC is used to process the data from the impedance analyzer.

2.2. Sample Preparation

Swine blood is utilized in this study instead of human blood because of the ethical and regulatory considerations. The swine blood is taken from a slaughterhouse within 12 h. A trisodium citrate solution with a concentration of 3.28% is injected into the swine blood with a volume ration of 1:9 to prevent blood clotting. Before the experiment, swine blood is put into the thermostatic water bath (HH-4, Jintan Chengdong Xinrui Instrument Factory, Changzhou, China) at 55 °C for 1 h to get the heated swine blood, which has been confirmed to be effective to mimic the burn injury for blood [24]. Then, the heated swine blood is put into the centrifuge to get the HRBCs, and normal swine blood is put into the centrifuge to get RBCs and plasma after centrifuging at 2000 × *g* rpm for 30 min under room temperature. Two experiments are designed to measure the difference between the electrical impedance characteristics of RBCs and HRBCs. As illustrated in Figure 1c, experiment is to mimic the blood with different burn injury degrees by mixing plasma with RBCs, HRBCs of different proportions. In the second experiment, plasma is mixed with RBCs to mimic the normal blood, as is shown in Figure 1d.

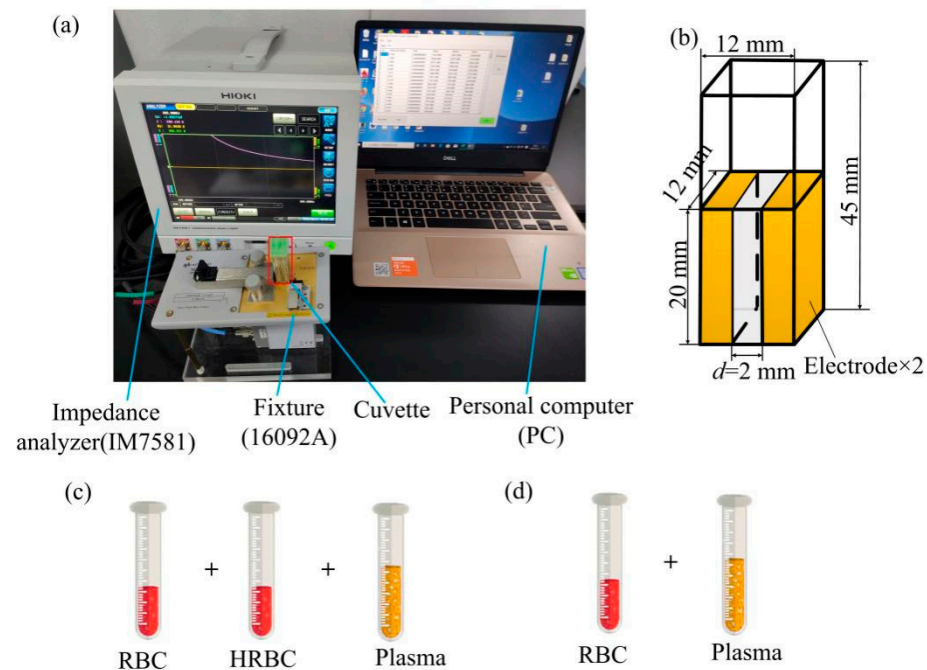


Figure 1. (a) Experimental setup; (b) structural dimension of the cuvette; (c) sample preparation of blood with different burn injury degrees (plasma, RBCs and HRBCs); (d) sample preparation of blood with different concentrations of RBCs.

2.3. Experimental Results

Figure 2a illustrates the experimental results about the impedance characteristics of blood with different proportions of HRBCs and RBCs measured by the system in Figure 1a. The experiments were carried out under the conditions of room temperature $t = 25\text{ }^{\circ}\text{C}$. By inserting different volumes of RBCs and HRBCs into plasma, the obtained H_{CT} is 0%, 10%, 20%, 30%, 40%, and H_{HCT} is 40%, 30%, 20%, 10%, 0% which ensures the value of ' $H_{CT} + H_{HCT}$ ' is always 40%. It has been reported that different degrees of burn injury bring different H_{CT} and H_{HCT} in blood [23]. Hence, the blood for the first experiment is mixed by different H_{CT} and H_{HCT} to mimic blood with different injury degrees. The experiments were taken under the sweeping frequency from $f = 100\text{ kHz}$ to $f = 300\text{ MHz}$ and the applied current of $I = 10\text{ mA}$. It is to note that because of the effect of inductance, some experimental data whose imaginary part of impedance is larger than 0 is going to be not shown in the figures. As shown in Figure 2a, the Nyquist plots of the blood with different H_{CT} and H_{HCT} all follow the classical shape of a semicircle: as frequency f goes up, the value of impedance increases at low frequencies and then it decreases after the characteristic frequency (peak point Z_t , the impedance under characteristic frequency f_c). To clearly clarify the electrical impedance characteristic variation, the peak point Z_t (Z_{Ret} , Z_{Imt}) of each Nyquist plot is investigated. Here, Z_{Ret} is the real part of impedance under the characteristic frequency f_c , Z_{Imt} is the imaginary part of impedance under the characteristic frequency f_c . The radius of the Nyquist plot has a negative correlation with H_{HCT} , and the value of Z_{Imt} reduces from $1.98\text{ }\Omega$ to $0.91\text{ }\Omega$ under the condition that H_{HCT} is from 0% to 40%. Moreover, as is seen in Figure 2b, the linear relationship between Z_{Imt} and H_{HCT} is shown as: $Z_{Imt} = -2.56 H_{HCT} + 2.01$ with a great linearity of $R^2 = 0.96$. Figure 2c shows the linear relationship between Z_{Ret} and H_{HCT} which is obtained as: $Z_{Ret} = -4.3 H_{HCT} + 12.16$ with a linearity of $R^2 = 0.91$. Compared with linearity of two relationships, Z_{Imt} is more sensitive to H_{HCT} . According to previous studies [23,25], H_{HCT} is related to the degrees of burn injury. It means that Z_{Imt} might be an effective parameter to detect the degree of burn injury.

In order to further investigate the parameter Z_{Imt} and the influence of HCT , the second experiment is conducted with the obtained HCT changing from $HCT = 20\%$ to $HCT = 80\%$. As shown in Figure 2c, the Nyquist plots of blood with different HCT also follow the shape of a semicircle. The radius of Nyquist plot increases under the condition that HCT enhances. Additionally, the value of Z_{Imt} climbs from 0.98Ω to 15.3Ω in the case that H_{HCT} jumps from 20% to 80% . The relationship between Z_{Imt} and HCT is shown as: $Z_{\text{Imt}} = 22.41 HCT + 5.68$ with a low linearity of $R^2 = 0.76$, which means Z_{Imt} is not so sensitive to HCT . Similarly, in Figure 2f, relationship between Z_{Ret} and HCT is shown as: $Z_{\text{Ret}} = 33.75 HCT + 0.45$ with a low linearity of $R^2 = 0.79$, which is also not sensitive to HCT . As a result, Z_{Imt} is confirmed to be effective to measure H_{HCT} , which means that it could be treated as a quantitative parameter to measure the degrees of burn injury.

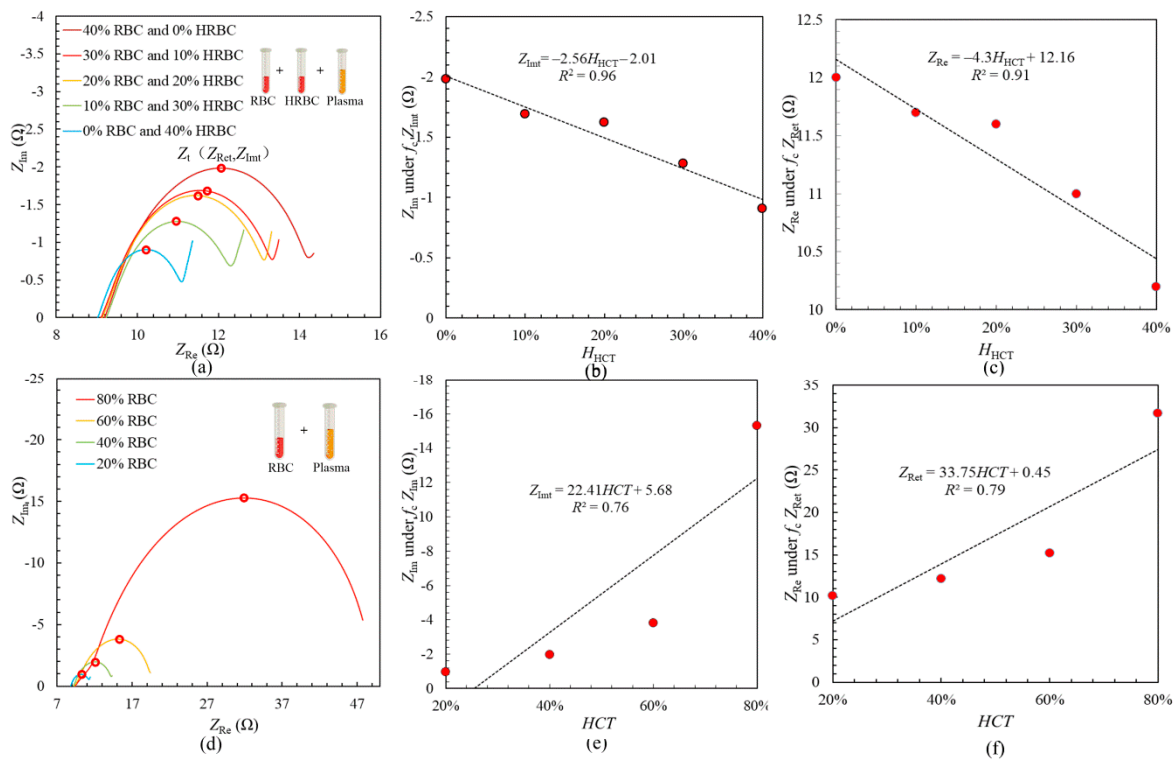


Figure 2. (a) The Nyquist plots of the blood with different HCT and H_{HCT} ; (b) Relationship between H_{HCT} and Z_{Imt} ; (c) Relationship between H_{HCT} and Z_{Ret} ; (d) The Nyquist plots of the blood with different HCT ; (e) Relationship between HCT and Z_{Imt} ; (f) Relationship between HCT and Z_{Ret} .

3. Discussion

3.1. Equivalent Circuit

In order to obtain the information of the electrical impedance properties of blood with different degrees of burn injury, the electrical impedance system is described by the seven-parameter equivalent circuit in Figure 3a. The blood system is divided into three parts: electrode polarization portion A, RBC polarization portion B and plasma portion C. R_1 is the electrolyte resistance; C_{RBC} is the RBC capacity, R_{RBC} is the resistance of RBC; R_p is the resistance of plasma and C_p is the capacitance of plasma. The impedance of the CPE is [26,27]:

$$Z_{\text{CPE}} = \frac{\cos(\frac{\pi}{2})p}{(2\pi f)^p T} - j \frac{\sin(\frac{\pi}{2})p}{(2\pi f)^p T} \quad (1)$$

where CPE is a ideal capacitor if p is close to 1 or a resistor if p is close to 0; t is the CPE constant, j is the imaginary unit, $2\pi f$ is angular frequency.

By taking the seven-parameter equivalent circuit, the fitting results in Figure 3b show that there is a great linear relationship between H_{HCT} and plasma resistance R_p . Table 1 shows the fitting parameters. The value of R_p goes up from $R_p = 3.93 \Omega$ to $R_p = 0.83 \Omega$ in the case that H_{HCT} increases from $H_{HCT} = 0\%$ to $H_{HCT} = 40\%$. Moreover, the relationship between R_p and H_{HCT} is obtained as: $R_p = -7.2H_{HCT} + 3.91$ with a linearity of $R^2 = 0.96$. This is thought to be caused by the fact that burn injury leads to the rupture of HRBCs. The capacitive properties of the cell membrane decreases after the rupture of HRBCs, and the hemoglobin inside cells escapes into the plasma which enhances the resistive properties of the plasma. From the proposed seven-parameter equivalent circuit, it is found that the parameter plasma resistance R_p is also effective to be applied as an indicator of burn injury degrees.

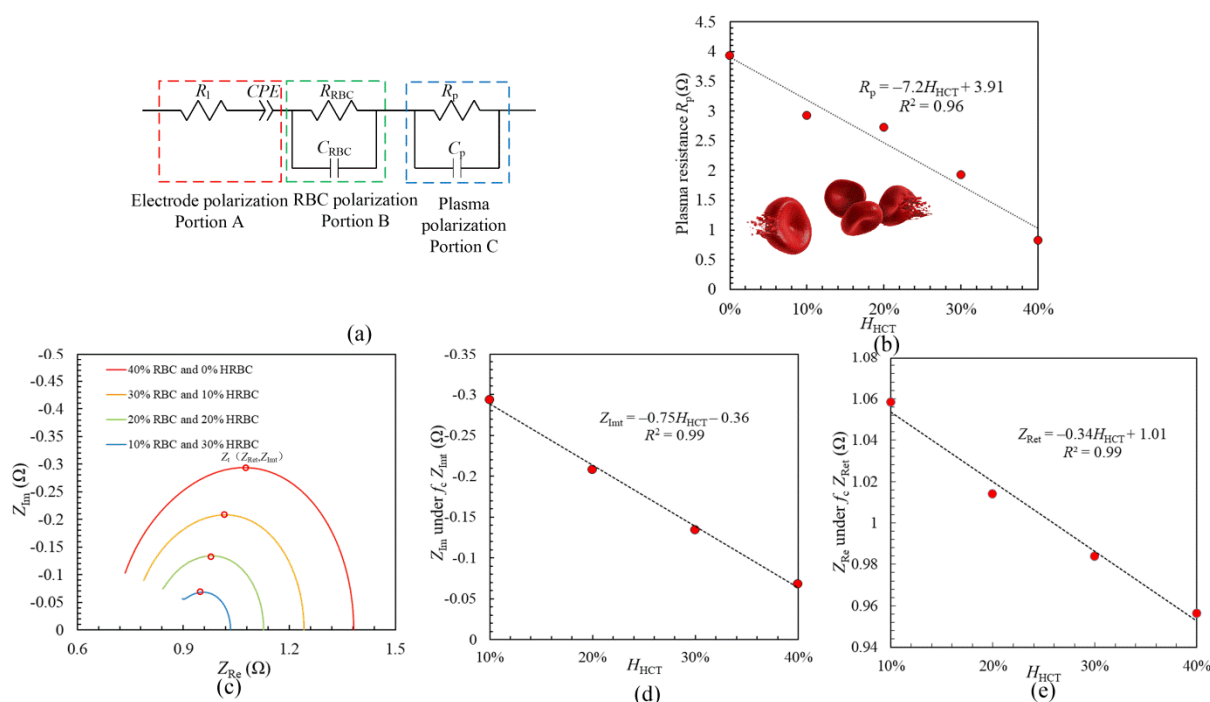


Figure 3. (a) Seven-parameter equivalent circuit of blood; (b) Fitting results: HRBC and relationship between H_{HCT} and R_p ; (c) The Nyquist plots of blood with different HCT and H_{HCT} ; (d) Relationship between H_{HCT} and Z_{im} ; (e) Relationship between H_{HCT} and Z_{re} .

Table 1. Fitting parameters.

H_{HCT} (-)	R_1 (Ω)	CPE_T ($F \cdot sec^{-0.28}$)	p_T (-)	R_{RBC} (Ω)	C_{RBC} (F)	R_p (Ω)	C_p (F)
40%	9.2	0.55	0.72	0.9	0.02	0.83	0.01
30%	9.2	0.55	0.72	0.8	0.01	1.93	0.02
20%	9.2	0.55	0.72	0.85	0.01	2.73	0.018
10%	9.2	0.55	0.72	0.75	0.01	2.93	0.02
0	9.2	0.55	0.72	0.5	0.005	3.93	0.01

3.2. Modified Hanai Equation

In this research, in order to quantitatively analyze the impedance variation of blood with different degrees of burn injury, traditional Hanai equation is modified for the theoretical calculation. Hanai equation is widely applied for the electrical impedance calculation in heterogeneous systems of dense colloids. The conventional Hanai equation has already been modified from the viewpoint of different proportions of RBCs and HRBCs. Moreover, from the previous experimental results in Section 2, the blood is simplified as the

solution of RBCs, HRBCs and plasma. The RBCs and HRBCs have been simplified as the 2-dimensional elliptical cells.

Here, modified Hanai equation with the elliptical model including all these influencing factors is calculated as follows:

$$\left(\frac{\varepsilon_{\text{plasma}}^{*T} - \varepsilon_{\text{RBC}}^*}{\varepsilon_{\text{plasma}}^* - \varepsilon_{\text{RBC}}^*}\right) \left(\frac{\varepsilon_{\text{plasma}}^{*T}}{\varepsilon_{\text{plasma}}^*}\right)^{-C_1} \left(\frac{\varepsilon_{\text{plasma}}^{*T} + A'\varepsilon_{\text{RBC}}^*}{\varepsilon_{\text{plasma}}^* + A'\varepsilon_{\text{RBC}}^*}\right)^{-C_2} \left(\frac{\varepsilon_{\text{plasma}}^{*T} + B'\varepsilon_{\text{RBC}}^*}{\varepsilon_{\text{plasma}}^* + A'\varepsilon_{\text{RBC}}^*}\right)^{-C_3} = 1 - HCT \quad (2)$$

$$\left(\frac{\varepsilon_{\text{blood}}^* - \varepsilon_{\text{HRBC}}^*}{\varepsilon_{\text{plasma}}^{*T} - \varepsilon_{\text{HRBC}}^*}\right) \left(\frac{\varepsilon_{\text{blood}}^*}{\varepsilon_{\text{plasma}}^{*T}}\right)^{-C_1} \left(\frac{\varepsilon_{\text{blood}}^* + A'\varepsilon_{\text{HRBC}}^*}{\varepsilon_{\text{plasma}}^{*T} + A'\varepsilon_{\text{HRBC}}^*}\right)^{-C_2} \left(\frac{\varepsilon_{\text{blood}}^* + B'\varepsilon_{\text{HRBC}}^*}{\varepsilon_{\text{plasma}}^{*T} + B'\varepsilon_{\text{HRBC}}^*}\right)^{-C_3} = 1 - H_{HCT} \quad (3)$$

where $\varepsilon_{\text{blood}}^*$ is the complex permittivity of blood, $\varepsilon_{\text{plasma}}^*$ is the complex permittivity of cell-free plasma and ε_{T}^* plasma is the complex permittivity of plasma with RBCs; $\varepsilon_{\text{RBC}}^*$ is the complex permittivity of RBC and $\varepsilon_{\text{HRBC}}^*$ is the complex permittivity of HRBC; A' and B' are the orientation factors influenced by RBCs orientation. C^1, C^2, C^3 are the deformation factors influenced by electrical field. ε_{m}^* is the relative permittivity of membrane. σ_{plasma} and σ_{m} are the conductivity of plasma and membrane, respectively. The other values based on the elliptical cell model have been described as:

$$\varepsilon_{\text{plasma}}^* = \varepsilon_{\text{plasma}} - j \frac{\sigma_{\text{plasma}}}{\omega \varepsilon_0} \quad (4)$$

$$\varepsilon_{\text{m}}^* = \varepsilon_{\text{m}} - j \frac{\sigma_{\text{m}}}{\omega \varepsilon_0} \quad (5)$$

Based on the modified Hanai equation [17], the impedance Z^* of blood is achieved according to Equation (6):

$$Z^* = \left(\frac{1}{d} j 2\pi f A \varepsilon_{\text{blood}}^*\right)^{-1} \quad (6)$$

where A is the area of the electrode of the container; d is the distance between the two electrodes of container, which is shown in Figure 1b.

3.3. Calculation Results

Figure 3c illustrates the calculation results of the impedance characteristics with different HCT and H_{HCT} based on the modified Hanai equation. The Nyquist plots of blood with different HCT and H_{HCT} all have semicircles, and the radius of the Nyquist plot reduces as H_{HCT} enhances. The value of impedance climbs at low frequencies and then it decreases after the characteristic frequency f_c (peak point Z_t). To clearly clarify the electrical impedance characteristic variation, the peak point Z_t (Z_{Ret} , Z_{Imt}) of each Nyquist plot is also investigated. The value of Z_{Imt} reduces from 0.29 Ω to 0.07 Ω under the condition that H_{HCT} goes up from 10% to 40% in the calculation results. Figure 3d illustrates Z_{Imt} is linearly related to H_{HCT} , moreover, the linear relationship between them is shown as $Z_{\text{Imt}} = -0.75H_{HCT} + 0.36$. This linear relationship has a great linearity of $R^2 = 0.99$. The linear relationship between Z_{Ret} and H_{HCT} is illustrated in Figure 3e as: $Z_{\text{Ret}} = -0.34H_{HCT} + 1.01$ with a great linearity of $R^2 = 0.99$. According to the calculation results in Figure 3 and the experimental results in Figure 2, it is confirmed that the parameter Z_{Imt} has a great linear relationship with H_{HCT} , which is effective to measure the degrees of burn injury quantitatively.

4. Conclusions

In this study, a quantitative and rapid burn injury detection method based on EIS has been proposed. The degrees of burn injury are estimated from the impedance values of blood with different HCT and H_{HCT} . Results show that the parameter Z_{Imt} and R_p are effective to be applied for the quantitative detection of burn injury. The linear relationship between Z_{Imt} and H_{HCT} could be obtained as $Z_{\text{Imt}} = -2.56H_{HCT} - 2.01$ with a high

approximation of $R^2 = 0.96$. Additionally, the linear relationship between plasma resistance R_p and H_{HCT} could be obtained as $R_p = -7.2H_{HCT} + 3.91$ with a high approximation of $R^2 = 0.96$. In the future, more work is still needed to make the practical application for burn injury patients.

Author Contributions: H.B.: Writing—original draft, data curation. J.L.: Writing—review & editing, Funding acquisition. J.W.: Conceptualization, Funding acquisition. L.C.: Data curation. Y.H.: Conceptualization, Review. Y.Z.: Conceptualization, Review. N.W.: Review, Funding acquisition. M.T.: Review. All authors have read and agreed to the published version of the manuscript.

Funding: This work was supported the Natural Science Foundation of Zhejiang Province: LY19E050010, LY20E050009 and LGF20E050001, and the General Research Projects of Zhejiang Provincial Department of Education: Y201943038.

Institutional Review Board Statement: The study was conducted according to the guidelines of the Declaration of Helsinki, and approved by the Institutional Review Board (or Ethics Committee) of Zhejiang Normal University (protocol code: 202001 and from 2021.01 to 2023.12).

Conflicts of Interest: The authors declare no conflict of interest.

References

1. François, P.; Rémi, G.; François, M.; Stéphane, T.; Josée, B. Continuous venovenous hemofiltration using customized replacement fluid for acute kidney injury with severe hypernatremia. *Clin. Kidney J.* **2016**, *9*, 540–542.
2. Priya, K.S.; Gnanamani, A.; Radhakrishnan, N.; Babu, M. Healing potential of *Datura alba* on burn wounds in albino rats. *J. Ethnopharmacol.* **2002**, *83*, 193–199. [[CrossRef](#)]
3. Upadhyay, N.; Kumar, K.R.; Mandotra, S.K.; Meena, R.N.; Siddiqui, M.S.; Sawhney, R.C.; Gupta, A. Safety and healing efficacy of Sea buckthorn (*Hippophae rhamnoides* L.) seed oil on burn wounds in rats. *Food Chem. Toxicol.* **2009**, *47*, 1146–1153. [[CrossRef](#)]
4. Monstrey, S.; Hoeksema, H.; Verbelen, J.; Pirayesh, A.; Blondeel, P. Assessment of burn depth and burn wound healing potential. *Burns* **2008**, *34*, 761–769. [[CrossRef](#)] [[PubMed](#)]
5. Heimbach, D.; Engrav, L.; Grube, B.; Marvin, J. Burn Depth: A Review. *World J. Surg.* **1992**, *16*, 10–15. [[CrossRef](#)]
6. Godina, M.; Derganc, M.; Brčić, A. The reliability of clinical assessment of the depth of burns. *Burns* **1977**, *4*, 92–96. [[CrossRef](#)]
7. Kahn, A.M.; McCrady, V.L.; Rosen, V.J. Burn wound biopsy multiple uses in patient management. *Scand. J. Plast. Recons.* **1979**, *13*, 53–56. [[CrossRef](#)]
8. Niazi, Z.B.M.; Essex, T.J.H.; Papini, R.; Scott, D.; McLean, N.R.; Black, M.J.M. New laser doppler scanner, a valuable adjunct in burn depth assessment. *Burns* **1993**, *19*, 485–489. [[CrossRef](#)]
9. Brink, J.A.; Sheets, P.W.; Dines, K.A.; Etchison, M.R.; Hanke, C.W.; Sadove, A.M. Quantitative assessment of burn Injury in porcine skin with high-frequency ultrasonic imaging. *Invest. Radiol.* **1986**, *21*, 645–651. [[CrossRef](#)]
10. Anand, G.; Lowe, A. Investigating electrical impedance spectroscopy for estimating blood flow-induced variations in human forearm. *Sensors* **2020**, *20*, 5333. [[CrossRef](#)]
11. Bruna, G.P.; David, C.M.; Pedro, B.F. Analytical Model for Blood Glucose Detection Using Electrical Impedance Spectroscopy. *Sensors* **2020**, *20*, 6928.
12. Wan, Y.; Su, Y.; Zhu, X.; Liu, G.; Fan, C. Development of electrochemical immunosensors towards point of care diagnostics. *Biosens. Bioelectron.* **2013**, *47*, 1–11. [[CrossRef](#)] [[PubMed](#)]
13. Xu, Y.; Xie, X.; Duan, Y.; Wang, L.; Cheng, Z.; Cheng, J. A review of impedance measurements of whole cells. *Biosens. Bioelectron.* **2016**, *77*, 824–836. [[CrossRef](#)]
14. Negahdary, M. Aptamers in nanostructure-based electrochemical biosensors for cardiac biomarkers and cancer biomarkers: A review. *Biosens. Bioelectron.* **2020**, *152*, 112018. [[CrossRef](#)] [[PubMed](#)]
15. Asami, K. Characterization of heterogeneous systems by dielectric spectroscopy. *Prog. Polym. Sci.* **2002**, *27*, 1617–1659. [[CrossRef](#)]
16. Li, J.; Sapkota, A.; Kikuchi, D.; Sakota, D.; Maruyama, O.; Takei, M. Red blood cells aggregability measurement of coagulating blood in extracorporeal circulation system with multiple-frequency electrical impedance spectroscopy. *Biosens. Bioelectron.* **2018**, *112*, 79–85. [[CrossRef](#)] [[PubMed](#)]
17. Li, J.; Wan, N.; Wen, J.; Cheng, G.; He, L.; Cheng, L. Quantitative detection and evaluation of thrombus formation based on electrical impedance spectroscopy. *Biosens. Bioelectron.* **2019**, *141*, 111437. [[CrossRef](#)]
18. DMishra, S.K.; Kumar, D.; Biradar, A.M.; Rajesh. Electrochemical impedance spectroscopy characterization of mercaptopropionic acid capped ZnS nanocrystal based bioelectrode for the detection of the cardiac biomarker—myoglobin. *Bioelectrochemistry* **2012**, *88*, 118–126. [[CrossRef](#)]
19. Nguyen, N.-V.; Jen, C.-P. Impedance detection integrated with dielectrophoresis enrichment platform for lung circulating tumor cells in a microfluidic channel. *Biosens. Bioelectron.* **2018**, *121*, 10–18. [[CrossRef](#)]
20. Ngoc, L.; Hien, T.; Kim, J.; Park, J.; Cho, S. A Review of Electrical Impedance Characterization of Cells for Label-Free and Real-Time Assays. *Biochip. J.* **2019**, *13*, 295–305. [[CrossRef](#)]

21. Hassan, Q.; Ahmadi, S.; Kerman, K. Recent Advances in Monitoring Cell Behavior Using Cell-Based Impedance Spectroscopy. *Micromachines* **2020**, *11*, 590. [[CrossRef](#)]
22. Sen, S.; Hsei, L.; Tran, N.; Romanowski, K.; Palmieri, T.; Greenhalgh, D.; Cho, K. Early clinical complete blood count changes in severe burn injuries. *Burns* **2018**, *45*, 97–102. [[CrossRef](#)]
23. Wu, Y.; Zhang, J.; Wu, J. Autoimmune hemolytic anemia occurred in burn patient: A case report. *Burns* **2014**, *40*, e9–e11. [[CrossRef](#)]
24. Grzelińska, E.; Bartosz, G.; Leyko, W.; Chapman, I.V. Effect of hyperthermia and ionizing radiation on the erythrocyte membrane. *Nt. J. Radiat. Biol.* **1982**, *42*, 45–55. [[CrossRef](#)]
25. Zahid, M.F.; Alsammak, M.S. Spurious thrombocytosis in the setting of hemolytic anemia and microcytosis secondary to extensive burn injury. *Turk. J. Hematol.* **2018**, *35*, 205–206. [[CrossRef](#)]
26. Shoar Abouzari, M.R.; Berkemeier, F.; Schmitz, G.; Wilmer, D. On the physical interpretation of constant phase elements. *Solid. State. Ionics* **2009**, *180*, 922–927. [[CrossRef](#)]
27. Zhbanov, A.; Yang, S. Electrochemical impedance spectroscopy of blood for sensitive detection of blood hematocrit, sedimentation and dielectric properties. *Anal. Methods.* **2017**, *9*, 3302–3313. [[CrossRef](#)]